Molecular Simulation of RMM: Ordered Mesoporous SBA-15 Type Material Having Microporous ZSM-5 Walls

C. G. Sonwane* and Q. Li

School of Chemical & Biomolecular Engineering, Georgia Institute of Technology, 311 Ferst Drive, Atlanta, Georgia 30332

Received: June 21, 2005; In Final Form: July 22, 2005

SBA-15 is a novel porous material with uniform size mesopores arranged in a regular pattern. The adjacent mesopores are connected to each other by microporous walls. The major disadvantages of these materials are that the walls are amorphous and have low thermal, hydrothermal, and mechanical stability. Recently, there have been a few attempts to either coat the walls of SBA-15 by microporous crystalline zeolites or to fabricate SBA-15 using CMK-3 in such a way that the walls are made up of ZSM-5. The present work provides a first-ever study of RMM (replicated mesoporous materials, which are SBA-15 like ordered mesoporous materials with walls made up of ZSM-5) using molecular modeling. A random orientation of the unit cells and the distribution of sizes of the supercells located at nucleation sites would be ideal to model the RMM. However, such a study would introduce more uncertainties with regard to voids between the individual supercells, noncrystalline silica, and the location of active sites where the nucleation occurs. In a simpler model studied in the present work, the walls of SBA-15 were made up of regularly arranged ZSM-5 having the same orientation. The structure was characterized by estimating the nitrogen accessible area/volume by Connolly surfaces, small-angle and wide-angle X-ray diffraction patterns, methane adsorption, and ice as a probe to study the pore structure. It was found that RMMs have significantly higher methane adsorption capacity compared to SBA-15 and the majority of methane is adsorbed in the microporous walls of RMM. Further research in the field of RMM is needed to obtain the details of zeolitic wall structure.

Introduction

The mesoporous molecular sieve SBA-15[6] has attracted significant attention because of its unique pore topology consisting of hexagonally arranged parallel mesopore channels where adjacent channels are connected by micropores present in the walls.[1,2,10−17] Such a structure provides an ideal reactor or catalyst where the mesopore channel acts as a pipe for transport of reactant without significant diffusion resistance and micropores in the walls provide activation sites for reactions. The mesopores in SBA-15 have a narrow pore size distribution, and pore size can be systematically modified with ease. However, the shape and size of pores present in the walls (could be either micropores or lower order mesopores) depend on the synthesis conditions and it may have a broad pore size distribution.[11,13,17]

SBA-15 has been used widely as a catalyst support and, more recently, in several other applications as a host. Some of its recent applications include use as an adsorbent for the removal of volatile organic compounds and toxic gases or as a chemical sensor,[17−20] as a host and carrier for antibiotics such as amoxicillin in pharmaceutical applications,[21] in the separation of light hydrocarbons[22] or the size-selective separation of proteins and vitamins,[23,24] as a host for biosensors,[25] for the separation of CO_2,[26] for catalytic conversion of fatty acids to gasoline,[27] and in the fabrication of membranes.[28]

The pore structure of SBA-15 materials is also being used for nanocasting or as a nanoreactor to synthesize a family of carbon-based[16] (or tungsten-based)[29] ordered nanoporous materials, CMK-3 and CMK-5. The high surface area and pore volume of these CMK materials make them potential candidates for other applications including methane/hydrogen storage,[30] catalysis,[31] and batteries.[32,33] Nanocasting is a process in which the microporous and mesopore cavity in SBA-15 is filled with guest reactant materials that may not react with the silicate walls directly, reaction is carried out, and later the SBA-15 casting is removed to obtain the product.

The main disadvantage of SBA-15 is that the walls are amorphous, causing their lower mechanical, thermal, and hydrothermal stability.[1−10,34] However, zeolites such as ZSM-5 have crystalline structures and higher stability. Therefore, a SBA-15 type material with the walls made up of ZSM-5 would be an ideal material answering stability-related problems. Recently, there have been attempts to either coat the walls of SBA-15 materials by zeolites by postsynthetic treatment[3−6] or make SBA-15 with walls made from zeolites using CMK-3 as a template.[1] Meynen et al.[6] deposited V−zeolite nanoparticles in SBA-15 using postsynthetic treatment. They found that the final material has higher microporosity (∼0.14 cm^3/g) than the original SBA-15 (∼0.1 cm^3/g). They also found that such a method gives rise to greater crystallinity of the SBA-15 walls. On et al.[3−5] found that the coating of SBA-15 by ZSM-5 using a postsynthesis route reduces the average diameter of SBA-15 from 7 to 5.4 nm; surface area is reduced from 800 to 465 m^2/g and pore volume is reduced from 1.56 to 0.78 cm^3/g. They found that the structure has higher mechanical, hydrothermal, and thermal stability. Sakthivel et al.[1] synthesized RMM (replicated mesoporous materials) having hexagonally ordered mesopores

* Corresponding author. Telephone: (763) 234-5738. Fax: (859) 406-3838. E-mail: shekar@nanoporous.com.

10.1021/jp053360n CCC: $30.25
Published on Web 08/25/2005

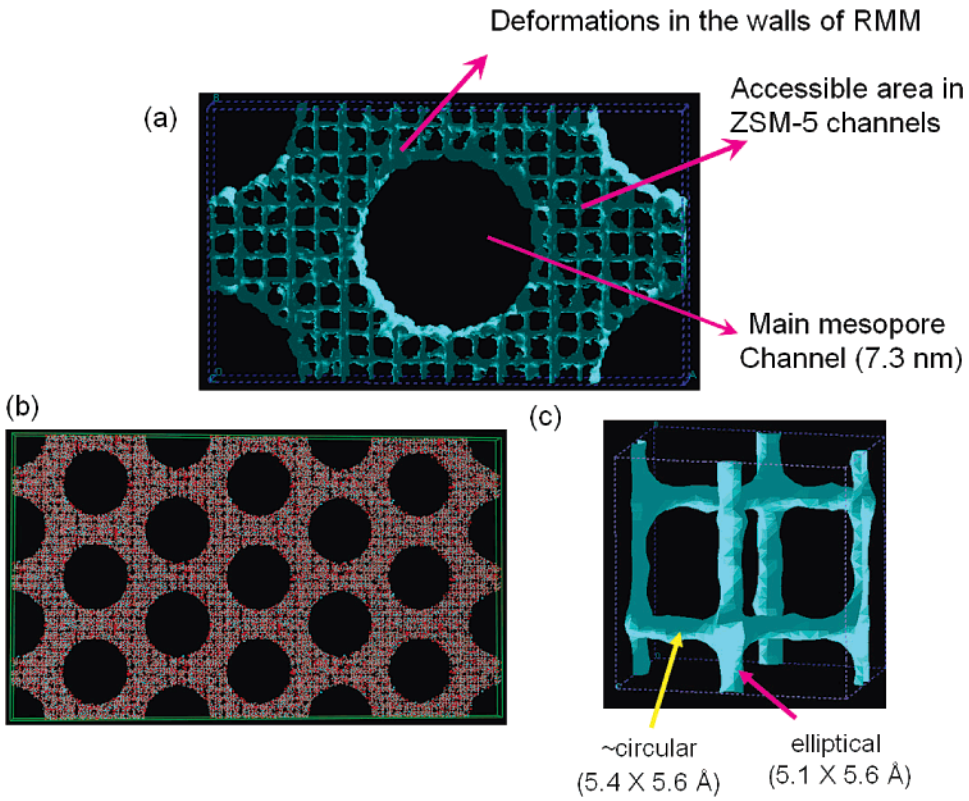

Figure 1. (a) Connolly surface area of RMM for nitrogen molecule; (b) 3 × 3 × 1 unit cell of RMM simulated in the present work; (c) Connolly surface area of ZSM-5 unit cell.

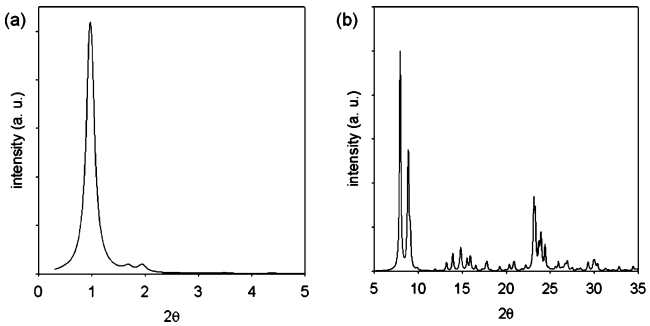

Figure 2. (a) Low-angle and (b) wide-angle simulated X-ray diffraction patterns of RMM.

similar to SBA-15, but the walls are made up of ZSM-5. They found that the RMMs contain 0.08 cm^3/g micropores (about 10% of the total pore volume). Also, it was reported that the RMMs have superior thermal, hydrothermal, and mechanical stability and improved acidic properties. There is an additional interesting route to formation of mesoporous materials with zeolite walls. Mesoporous materials with walls made from zeolites can be formed by a direct synthesis route using zeolite precursor as a silicon source.[7−9] These studies indicate that new kinds of porous materials with bimodal distribution having a narrow distribution of both micropores and mesopores are possible to synthesize.

Leading researchers such as Seaton,[35,36] Schuth,[37,38] Neimark,[39] Feutson,[40] Koh,[41,42] Solovyov,[43] Kutchta,[44] Cao,[45] Coasne,[46] Kleestorfer,[47] Gubbins,[48] Bhatia,[49,50] and co-workers in the area of application of computational methods for the study of micro- and mesoporous materials have mainly investigated MCM-41 or similar model materials, properties, and their applications. In addition, the models are too simple to account for minute details at micro- and macroscopic levels. Some of the models assume MCM-41 to be a smooth cylinder,[39] and others relate MCM-41 to a quartz silica tube[35,36] or a structure made up of purely O atoms.[48] The new ordered materials such as RMM have brought several new features which were not available in the existing materials. To the best of my knowledge, there has been no single attempt to model RMM.

In the present work, we have presented a study of RMM materials using molecular modeling. The structure was characterized using simulated small-angle and wide-angle X-ray diffraction, accessible surface area by the Connolly method, methane adsorption, and ice probing.

Simulation Details

The RMMs of two different pore sizes (5.5 and 7.3 nm) were fabricated by placing the atoms on a ZSM-5 supercell as shown in Figure 1b. A random orientation of the unit cells and the distribution of sizes of the supercells would be ideal to model the RMM. However, such a study would introduce more uncertainties with regard to voids between the individual supercells, noncrystalline silica, and the location of active sites where the nucleation occurs. At the moment, insufficient details of the wall structure of RMM are available in the literature. Further studies with wide-angle X-ray as well as small-angle X-ray diffraction, positron annihilation, and helium pycnometry are needed to study the details of the wall structure. Before attempting such a complex study, it is worthwhile to study a less complex scenario where all the unit cells are oriented in the same direction and they are made from a single supercell. ZSM-5 pore structure consists of interconnecting micropore channels where one is elliptical (5.1 × 5.6 Å) and the other is near circular in cross section (5.4 × 5.6 Å). More details of pore structure and the ordering of the atoms have been widely studied, and the reader is encouraged to follow standard textbooks (e.g., Ruthven[51]) or use the Internet search engine Google with the keyword "ZSM-5". In experimental synthesis

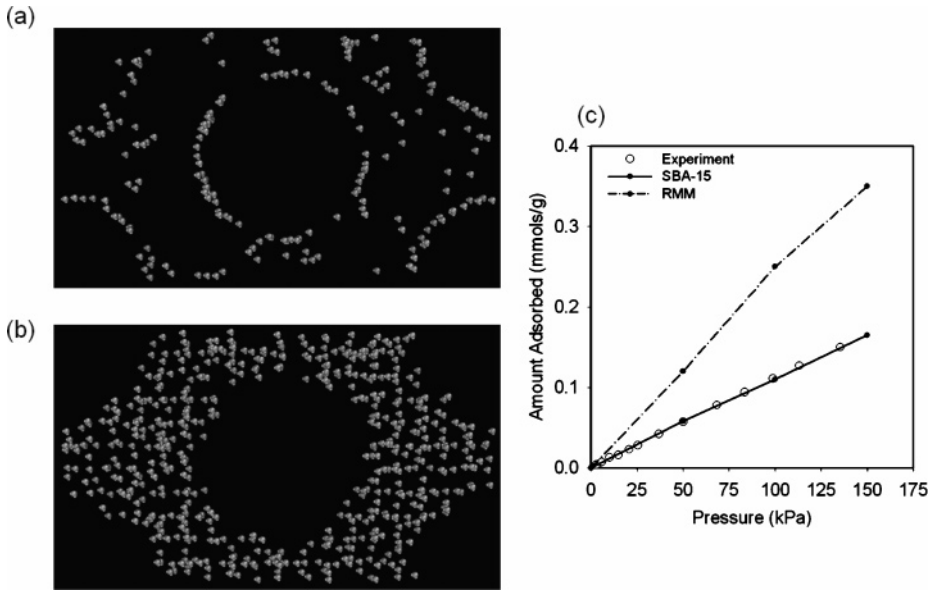

Figure 3. Methane adsorption in SBA-15 and RMM. Snapshots of methane adsorbed in (a) SBA-15 and (b) RMM. (c) Comparison of simulated methane adsorbed in SBA-15 and RMM with experimental SBA-15 results.

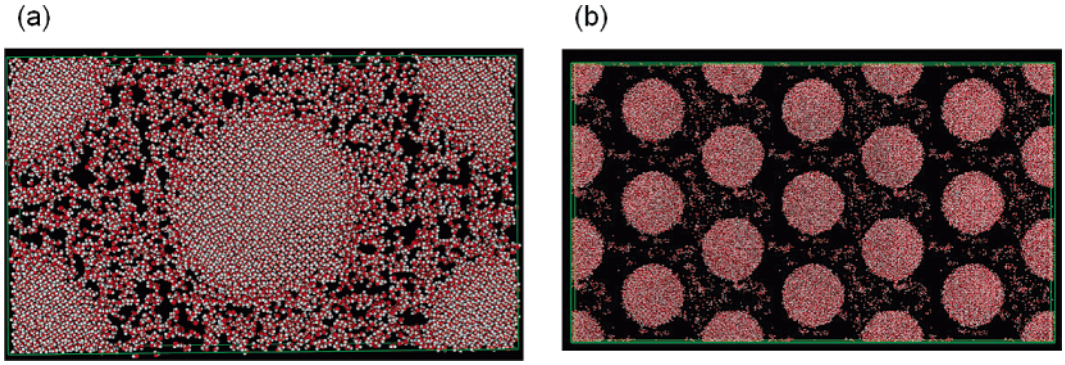

Figure 4. Ice as a probe to study the pore structure of RMM and SBA-15: equilibrated structure of ice in RMM and SBA-15. The wall structure is removed and only ice is shown for better visualization.

RMMs are made using CMK-3 as a template. In the present simulation, we used dummy carbon rods (one at the center and one-fourth of each at each corner of the hexagonal lattice). The atoms of the zeolite supercell lying in the template were removed. All the unpaired atoms near the cavities or the template were terminated with H.

The structure was optimized and then equilibrated at 300 K by NVT to obtain the minimum energy configuration. The details of the procedure are provided in our earlier articles.[53,54] We provide here relevant details. The mmff94x force field[55] was used, and a step size of 2 fs was chosen. The entire structure was equilibrated for 100 ps or more until the temperature remained constant (within 10 deg) in NVE simulations. The shape of the cavities in the final structure was no longer perfectly spherical.

The simulations and small- as well as wide-angle X-ray characterization were performed using MOE[55] and Cerius2[56] packages. The experimental details available in the literature[1,2] are not sufficient to model the micro- and mesostructure of RMM. Therefore, on several occasions, the properties or the method of simulating SBA-15 was extended here for RMM materials. It is expected that the walls of RMM consists of small units of ZSM-5 with different sizes and random orientations. The space between these supercells gives rise to voids. The size and distribution of such voids need to be investigated using experimental studies. In the present simulations, to introduce deformations in the walls, the spherical cavities (with Gaussian distribution with 0.7 nm mean and 0.2 nm standard deviation) were inserted by removing atoms at randomly selected places.

Results and Discussion

The accessible area of SBA-15 and ZSM-5 unit cells for nitrogen molecules was estimated by using the Connolly procedure[57] as shown in parts a and c, respectively, of Figure 1. The visualization of a 3 × 3 × 1 structure of SBA-15 is shown in Figure 1b. The unit cell parameters are 18.18 nm × 10.5 nm × 4 nm, while the diameter of the main mesopore channels is 7.3 nm. The surface area of the structure was found to be 650 m^2/g, which is less than that of the parent SBA-15 structure (~800 m^2/g). The apparent decrease is probably due to the higher density of walls made from ZSM-5 zeolite. The total pore volume of pure ZSM-5 is 0.15 cm^3/g (which is predominantly micropore volume), compared to the total pore volume of 0.9 cm^3/g of pure SBA-15. Also, the surface area of ZSM-5 is 100−200 m^2/g, compared to the total surface area of 800 m^2/g of pure SBA-15. This simulation result is consistent with the experimental results of Sakthivel et al.,[1] who reported that the BET area of RMM is 550−600 m^2/g, which is lower than that of pure SBA-15. The simulated X-ray diffraction patterns are shown in Figure 2. The low-angle XRD pattern in Figure 2a resembles the experimental XRD pattern of RMMs reported by Sakthivel et al.[1] The simulated wide-angle X-ray

pattern shown in Figure 2b shows that the walls are made of ZSM-5. A comparison of such patterns with experiments leads us to two independent studies. In the first, Sakthivel et al.[1] did not find any WAXS patterns. The main reason was because the zeolite particles were smaller than 5 nm and therefore not detectable in X-ray diffraction. However, Mokaya and co-workers[2] have synthesized such materials and found that the WAXS patterns of these materials match closely the ZSM-5. Therefore, further experimental study in this regard is needed to ascertain the wall structure of RMM. The simulated materials presented here have a uniform orientation and are part of a large supercell. We have deformation present in the walls in the form of spherical cavities (with Gaussian distribution of mean = 0.7 nm and standard deviation = 0.3 nm). The most accurate simulation model for RMM would involve randomly oriented supercells of ZSM-5 with a broad size range present in the walls of RMM. However, such a simulation study would require experimental knowledge of the size distribution of ZSM-5 crystals and voids present between the adjacent crystals. We are currently investigating such a model.

The grand canonical Monte Carlo (GCMS) simulation of adsorption of methane carried out on parent SBA-15 and RMM at 303 K over a pressure range of 0−150 kPa was studied, and it is shown in Figure 3. For comparison with simulations, the experimental results on pure SBA-15[18] are also shown in Figure 3c. It can be seen from the snapshots in Figure 3a,b that in RMMs the methane adsorption occurs mainly in the ZSM-5 pores and the number of methane molecules adsorbed per unit cell of the RMM is much higher than in the SBA-15. In SBA-15, the adsorption occurs on the surface and a small quantity is adsorbed in the micropores. The micropores in SBA-15 walls have no definite shape and could range from 0.5 to 3 nm in size. In the SBA-15 model[54] used in the present work, the individual micropores were spherical cavities with a mean size of 0.7 nm. However, joining of two or more adjacent cavities could give rise to larger voids. These larger voids do not have stronger potential and have less adsorption of methane. The results shown in Figure 3c indicate that the methane adsorption in RMM per unit cell is much higher than in the corresponding SBA-15.

The pore structure of the RMM and SBA-15 was studied by modeling the ice inside the micropores as well as mesopores. The H_2O molecules were placed inside the empty space of the RMM model to match the density of ice, the RMM structure was fixed, and the H_2O molecules were allowed to freely move in the pores. The system was optimized and equilibrated at 273 K for more than 100 ps. Snapshots of the ice (after removing the RMM or SBA-15) are shown in Figure 4a (for RMM) and Figure 4b (for SBA-15). The H_2O molecules present in the main mesopore channel as well as the walls of RMM (in ZSM-5 pores) can be seen from Figure 4. The water molecules present in the walls of RMM are significantly larger compared to the those in SBA-15. The main reason for this is the presence of a highly networked structure in RMM.

In summary, we have studied the structure and properties of RMM, a recently invented micro- and mesoporous molecular sieve using molecular modeling. The methane adsorbed in the RMM is significantly higher than that in the parent SBA-15, and the majority of adsorption occurs in the microporous ZSM-5 walls of RMMs.

Acknowledgment. The authors acknowledge Professor Pete Ludovice, Professor Chris Jones, Professor Jennifer Wilcox, Professor Ed Ma, John Richardson, Andrew Swann, and Robert John Caulkins for useful discussions and help. The early development of the work was funded by a grant of US DOE Office of Basic Energy Sciences through Catalysis Science Contract No. DE-FG02-03ER15459 (GT-UVA Focused Program in Catalysis by Immobilized Organometallics, Director and Principle Investigator (PI): Professor Christopher W. Jones and co-PI: Professor Peter J. Ludovice).

References and Notes

(1) Sakthivel, A.; Huang, S.-J.; Chen, W.-H.; Chen, W.-H.; Lan, Z.-H.; Chen, K.-H.; Kim, T.-W.; Ryoo, R.; Chiang, A. S. T.; Liu, S.-B. *Chem. Mater.* **2004**, *16*, 3168.

(2) Yang, Z.; Xia, Y.; Mokaya, R. *Adv. Mater.* **2004**, *16*, 727.

(3) Do, T.-O.; Nossov, A.; Springuel-Huet, M.-A.; Schneider, C.; Bretherton, J. L.; Fyfe, C. A.; Kaliaguine, S. *J. Am. Chem. Soc.* **2004**, *126*, 14324.

(4) Do, T.-O.; Kaliaguine, S. *Angew. Chem.* **2002**, *114*, 1078.

(5) Do, T.-O.; Kaliaguine, S. *Angew. Chem., Int. Ed.* **2001**, *40*, 3248.

(6) Meynen, V.; Beyers, E.; Cool, P.; Vansant, E. F.; Mertens, M.; Weyten, H.; Lebedev, O. I.; Tendeloo, G. V. *Chem. Commun.* **2004**, 898.

(7) Han, Y.; Xiao, F.-S.; Wu, S.; Sun, Y.; Meng, X.; Li, D.; Lin, S.; Deng, F.; Ai, X. *J. Phys. Chem. B* **2001**, *105*, 7963.

(8) Liu, Y.; Pinnavaia, T. *J. Chem. Mater.* **2002**, *14*, 3.

(9) Han, Y.; Wu, S.; Sun, Y.; Li, D.; Xiao, F.-S.; Liu, J.; Zhang, X. *Chem. Mater.* **2002**, *14*, 1144.

(10) Zhao, D. Y.; Huo, Q. S.; Feng, J. L.; Chmelka, B. F.; Stucky, G. D. *J. Am. Chem. Soc.* **1998**, *120*, 6024.

(11) Kruk, M.; Jaroniec, M.; Kim, T.-W.; Ryoo, R. *Chem. Mater.* **2003**, *15*, 2815.

(12) Liu, J.; Zhang, X.; Han, Y.; Xiao, F.-S. *Chem. Mater.* **2002**, *14*, 2536.

(13) Goltner, C. G.; Smarsly, B.; Berton, B.; Antonietti, M. *Chem. Mater.* **2001**, *13*, 1617.

(14) Miyazawa, K.; Inagaki, S. *Chem Commun.* **2000**, 2121.

(15) Galarneau, A.; Cambon, H.; Renzo, F. D.; Fajula, F. *Langmuir* **2001**, *17*, 8328.

(16) Jun, S.; Joo, S. H.; Ryoo, R.; Kruk, M.; Jaroniec, M.; Liu, Z.; Ohsuna, T.; Terasaki, O. *J. Am. Chem. Soc.* **2000**, *122*, 10712.

(17) Ueno, Y.; Tate, A.; Niwa, O.; Zhou, H.-S.; Yamada, T.; Honma, I. *Chem. Commun.* **2004**, *6*, 746.

(18) Yamada, T.; Zhou, H.-S.; Uchida, H.; Honma, I.; Katsube, T. *J. Phys. Chem. B* **2004**, *108*, 13341.

(19) Xu, Y.; Jiang, Q.; Cao, Y.; Wei, Y. L.; Yun, Z. Y.; Xu, J. H.; Wang, Y.; Zhou, C. F.; Shi, L. Y.; Zhu, J. H. *Adv. Funct. Mater.* **2004**, *14*, 1113.

(20) Hudson, M. J.; Knowles, J. P.; Harris, P. J. F.; Jackson, D. B.; Chinn, M. J.; Ward, J. L. *Microporous Mesoporous Mater.* **2004**, *75*, 121.

(21) Vallet-Regi, M.; Doadrio, J. C.; Doadrio, A. L.; Izquierdo-Barba, I.; Perez-Pariente, J. *Solid State Ionics* **2004**, *172*, 435.

(22) Newalkar, B. L.; Choudary, N. V.; Turaga, U. T.; Vijayalakshmi, R. P.; Kumar, P.; Komarneni, S.; Bhat, T. S. G. *Chem. Mater.* **2003**, *15*, 1474.

(23) Katiyar, A.; Ji, L.; Smirniotis, P.; Pinto, N. G. *J. Chromatogr., A* **2005**, *1069*, 119.

(24) Hartmann, M.; Vinu, A.; Chandrasekar, G. *Chem. Mater.* **2005**, *17*, 829.

(25) Shiotsuka, H.; Imamura, T.; Nomoto, T.; Ogawa, M. *PCT Int. Appl.* **2005**, *121*, WO 2005016971.

(26) Gray, M. L.; Soong, Y.; Champagne, K. J.; Pennline, H. W.; Baltrus, J.; Stevens, R. W., Jr.; Khatri, R.; Chuang, S. S. C. *Int. J. Environ. Technol. Manage.* **2004**, *4*, 82.

(27) Ooi, Y.-S.; Zakaria, R.; Mohamed, A. R.; Bhatia, S. *Energy Fuels* **2005**, *19*, 736.

(28) Lu, Q.; Gao, F.; Komarneni, S.; Mallouk, T. E. *J. Am. Chem. Soc.* **2004**, *126*, 8650.

(29) Yue, B.; Tang, H.; Kong, Z.; Zhu, K.; Dickinson, C.; Zhou, W.; He, H. *Chem. Phys. Lett.* **2005**, *407*, 83.

(30) Zhou, H.; Zhu, S.; Honma, I.; Seki, K. *Chem. Phys. Lett.* **2004**, *396*, 252.

(31) Lu, A.-H.; Schmidt, W.; Matoussevitch, N.; Boennemann, H.; Spliethoff, B.; Tesche, B.; Bill, E.; Kiefer, W.; Schueth, F. *Angew. Chem., Int. Ed.* **2004**, *43*, 4303.

(32) Fan, J.; Wang, T.; Chengzhong, Y.; Bo, T.; Zhiya, J.; Zhao, D. *Adv. Mater.* **2004**, *16*, 1432.

(33) Zhou, H.; Zhu, S.; Hibino, M.; Honma, I.; Ichihara, M. *Adv. Mater.* **2003**, *15*, 2107.

(34) Sonwane, C. G.; Li, Q. *J. Phys. Chem. B* **2005**, *109*, 5691.

(35) He, Y.; Seaton, N. *Langmuir* **2003**, *19*, 10132.

(36) Yun, J.-H.; Duren, T.; Keil, F. J.; Seaton, N. A. *Langmuir* **2002**, *18*, 2693.

(37) Sauer, J.; Marlow, F.; Schuth, F. *Phys. Chem. Chem. Phys.* **2001**, *3*, 5579.
(38) Schacht, S.; Janicke, M.; Schuth, F. *Microporous Mesoporous Mater.* **1998**, *22*, 485.
(39) Ravikovitch, P. I.; Wei, D.; Chueh, W. T.; Haller, G. L.; Neimark, A. V. *J. Phys. Chem. B* **1997**, *101*, 3671.
(40) Feutson, B. P.; Higgins, J. B. *J. Phys. Chem.* **1994**, *98*, 4459.
(41) Koh, C. A.; Westacott, R. E.; Nooney, R. I.; Boissel, V.; Tahir, S. F.; Tricarico, V. *Mol. Phys.* **2002**, *100*, 2087.
(42) Koh, C. A.; Montanari, T.; Nooney, R. I.; Tahir, S. F.; Westacott, R. E.; *Langmuir* **1999**, *15*, 6043.
(43) Solovyov, L. A.; Kirik, S. D.; Shmakov, A. N.; Romannikov, V. N. *Microporous Mesoporous Mater.* **2001**, *44*, 17.
(44) Kuchta, B.; Llewellyn, P.; Denoyel, R.; Firlej, L. *Colloids Surf., A* **2004**, *241*, 137.
(45) Cao, D.; Shen, Z.; Chen, J.; Zhang, X. *Microporous Mesoporous Mater.* **2004**, *67*, 159.
(46) Coasne, B.; Pellenq, R. J.-M. *J. Chem. Phys.* **2004**, *120*, 2913.
(47) Kleestorfer, K.; Vinek, H.; Jentys, A. *J. Mol. Catal., A* **2001**, *166*, 53.
(48) Maddox, M. W.; Gubbins, K. E. *Langmuir* **1997**, *13*, 1737.
(49) Bhatia, S. K.; Nicholson, D. *Phys. Rev. Lett.* **2003**, 016105/1−016105/4.
(50) Sonwane, C. G.; Bhatia, S. K.; Calos, N. *Ind. Eng. Chem. Res.* **1998**, *37*, 2271.
(51) Ruthven, D. *Principles of Adsorption and Adsorption Processes*; Wiley: New York, 1984.
(52) Sonwane, C. G.; Ludovice, P. J. *J. Mol. Catal., A: Chem.* **2005**, *238*, 135.
(53) Sonwane, C. G.; Jones, C. W.; Ludovice, P. J. Submitted for publication in *J. Phys. Chem B.*
(54) Sonwane, C. G.; Richardson, J. M.; Jones, C. W.; Ludovice, P. J. To be submitted to *Microporous Mesoporous Mater.* **2005**.
(55) MOE, Molecular Operating Environment; Chemical Computing Group Inc.; Release 2004.03.
(56) Cerius2 Modeling Environment, Release 4.6; Accelrys.
(57) Connolly, M. L. *J. Appl. Crystallogr.* **1983**, *16*, 548.